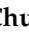*Article*

A Tailored Biomimetic Hydrogel as Potential Bioink to Print a Cell Scaffold for Tissue Engineering Applications: Printability and Cell Viability Evaluation

Shyuan-Yow Chen [1], Yung-Chieh Cho [2,3,†], Tzu-Sen Yang [4], Keng-Liang Ou [2,5,6,7,8,*], Wen-Chien Lan [6], Bai-Hung Huang [2,9,10], Takashi Saito [7], Chi-Hsun Tsai [7], Bou-Yue Peng [3,11,*], Yen-Chun Chuo [2,12], Hung-Yang Lin [13], Hsiao-Wei Chao [14], Christopher J. Walinski [15] and Muhammad Ruslin [16]

[1] Department of Dentistry, Cathay General Hospital, Taipei 106, Taiwan; shyuanyc@ms8.hinet.net
[2] Biomedical Technology R & D Center, China Medical University Hospital, Taichung 404, Taiwan; D204106003@tmu.edu.tw (Y.-C.C.); T33782@mail.cmuh.org.tw (B.-H.H.); m249108001@tmu.edu.tw (Y.-C.C.)
[3] School of Dentistry, College of Oral Medicine, Taipei Medical University, Taipei 110, Taiwan
[4] Graduate Institute of Biomedical Optomechatronics, College of Biomedical Engineering, Taipei Medical University, Taipei 110, Taiwan; tsyang@tmu.edu.tw
[5] Department of Dentistry, Taipei Medical University-Shuang Ho Hospital, New Taipei City 235, Taiwan
[6] Department of Oral Hygiene Care, Ching Kuo Institute of Management and Health, Keelung 203, Taiwan; jameslan@ems.cku.edu.tw
[7] Division of Clinical Cariology and Endodontology, Department of Oral Rehabilitation, School of Dentistry, Health Sciences University of Hokkaido, Hokkaido 061-0293, Japan; t-saito@hoku-iryo-u.ac.jp (T.S.); e526095019@tmu.edu.tw (C.-H.T.)
[8] 3D Global Biotech Inc. (Spin-off Company from Taipei Medical University), New Taipei City 221, Taiwan
[9] Asia Pacific Laser Institute, New Taipei City 220, Taiwan
[10] Implant Academy of Minimally Invasive Dentistry, Taipei 106, Taiwan
[11] Division of Oral and Maxillofacial Surgery, Department of Dentistry, Taipei Medical University Hospital, Taipei 110, Taiwan
[12] School of Dental Technology, College of Oral Medicine, Taipei Medical University, Taipei 110, Taiwan
[13] Department of Dentistry, Fu Jen Catholic University Hospital, Fu Jen Catholic University, New Taipei City 243, Taiwan; a00207@mail.fjuh.fju.edu.tw
[14] Department of Dentistry, University of Debrecen, 4032 Debrecen, Hungary; mchaochao37@gmail.com
[15] Department of Dental Medicine, Touro College of Dental Medicine, Hawthorne, NY 10532, USA; christopher.walinski@touro.edu
[16] Department of Oral and Maxillofacial Surgery, Faculty of Dentistry, Hasanuddin University, Makassar 90245, Indonesia; mruslin@unhas.ac.id
* Correspondence: klou@tmu.edu.tw (K.-L.O.); pemg@tmu.edu.tw (B.-Y.P.)
† Co-First author: Yung-Chieh Cho.

Abstract: The present study established a maximum standard for printing quality and developed a preliminary ideal index to print three-dimensional (3D) construct using the Gly-Arg-Gly-Asp (GRGD) peptide modified Pluronic-F127 hydrogel (hereafter defined as 3DG bioformer (3BE)) as bioink. In addition, the biocompatibility of 3BE for 3D printing applications was carefully investigated. For biocompatibility study and ideal printing parameter, we used the formulation of 3BE in three different concentrations (3BE-1: 25%, 3BE-2: 30%, and 3BE-3: 35%). The 3BE hydrogels were printed layer by layer as a cube-like construct with all diameters of the needle head under the same feed (100 mm/s). The printing parameters were determined using combinations of 3BE-1, 3BE-2, and 3BE-3 with three different standard needle sizes (Φ 0.13 mm, Φ 0.33 mm, and Φ 0.9 mm). The printed constructs were photographed and observed using optical microscopy. The cell viability and proliferation were evaluated using Live/Dead assay and immunofluorescence staining. Results showed that a stable of printed line and construct could be generated from the 3BE-3 combinations. Cytotoxicity assay indicated that the 3BE hydrogels possessed well biocompatibility. Bioprinting results also demonstrated that significant cell proliferation in the 3BE-3 combinations was found within three days of printing. Therefore, the study discovered the potential printing parameters of 3BE as bioink to print a stable construct that may also have high biocompatibility for cell encapsulation. This finding could serve as valuable information in creating a functional scaffold for tissue engineering applications.

1. Introduction

One of the utmost purposes of research in tissue engineering and regenerative medicine is to create tissue/organ mimicking the natural structure of the human body for utilization in organ transplantation therapies [1–3]. Recently, three-dimensional (3D) bioprinting has emerged as a key approach in designing and constructing artificial tissue/organ [4–7]. This technology incorporates various cells, growth factors, and biomaterials to generate biomedical constructs in which the cell aggregates are deposited layer-by-layer with a supportive matric bioink [8–10]. In the frame of biological field, hydrogel has been suggested as an ideal material for bioink due to its high biocompatibility, low cytotoxicity, and structural resemblance to the extracellular matrix [11–13]. However, applying hydrogels in bioprinting technology may be troublesome since it requires suitable mechanical properties and gelation characteristics to support a steady deposition from the printer [14]. Besides, the fact that not every hydrogel is repeatable to proceed by the printer leads to the quantification of hydrogel printability, which is sometimes rough and resulting in lack of hydrogel bioink [6,8]. Furthermore, a major obstacle to achieve a better encapsulation of cells and maintain cell viability after 3D printing procedure still present as challenging issues to be resolved [6,10,15]. Due to these facts, the improvement of a printable hydrogel that can maintain a stable structure and facilitate the growth and function of the cell is demanded to escalate the existing approach in tissue engineering [7,12,16].

The 3D printed construct and cell viability are known to be directly influenced by materials used for bioink and bioprinting parameters [13,16]. Recently, a thermo-sensitive polymer, so-called Pluronic-F127 (F127), has been known to possess promising properties for 3D bioprinting and tissue engineering applications [7,17]. This material can be moved and shifted simply due to its micellar-packing gelation characteristic [18]. The F127 has a broad range of sol-gel transition temperature (10–40 °C), resulting in a stable viscosity at room temperature and human body temperature [13,18,19]. The reversible properties of F127 can be useful in producing complex and stable 3D cell-laden with high resolution of the printed constructs [4]. It can be easily printed without excessive stress for the encapsulated cells and can be simply washed away from the target structure after printing [20,21]. Most importantly, this material is regarded as one of the best types of printable hydrogels for cell printing applications owing to its inert properties towards various cell types [19,20]. In addition to the F127, Arg-Gly-Asp (RGD) peptide has also attracted particular interest in 3D cell culture for promoting cell growth and proliferation [22–24]. RGD is an integrin binding site, which belongs to the class of adhesive proteins [25]. RGD region is found in various proteins, and is crucial for facilitating cell-adhesive activity. Moreover, it has been demonstrated that the Gly-Arg-Gly-Asp (GRGD) peptide sequence is identical to the cell-binding region of fibronectin protein [26]. Accordingly, it would be beneficial if F127 could be developed as bioink by the modification of GRGD peptide to enhance cell growth and proliferation activity.

Not only materials used for bioink, but also ideal printing parameters, particularly positioning and printing resolution, are important aspects for successful bioprinting results [16]. Previously, the increase of polymer concentration was a primary approach to enhance the printability of hydrogels. Unfortunately, this method entails precise control over the deposition process [18,27]. Sometime there will be a fine balance between printing parameters such as printing speed, nozzle diameter, and temperature, which can affect the result of bioprinting, especially when printing the cell-laden with hydrogels. The distinct properties in each type of hydrogels caused the optimization of particular hydrogel compositions such as polymer concentrations and crosslinking densities, which need to be fully understood [14]. To address these issues, it is pivotal to thoroughly investigate the different printing parameters suitable to print a specific material such as hydrogels [17,28].

In the present study, we investigated the printability of the Gly-Arg-Gly-Asp (GRGD) peptide modified F127 hydrogel (hereafter defined as 3DG bioformer (3BE)) as bioink. We determined the stable printing quality and developed a preliminary ideal index to print a 3D construct using various concentrations of 3BE by means of a self-fabricated 3D bioprinting system. In addition, we presented the initial cell viability of fibroblasts inside the 3BE in 3D printed constructs. We believe that by using these parameters and combining specific cell types with 3BE as bioink, we could potentially create any configuration of a complex scaffold that mimics natural tissues/organs for tissue engineering and organ regenerative applications.

2. Materials and Methods

2.1. Preparation of the Investigated Hydrogels

The investigated material in the present study used a high-purity F127 polymer (Pluronic®F127; Sigma 0.709 mmol, Taipei, Taiwan) that was modified by GRGD peptide (RDD Lab. Inc., New Taipei City, Taiwan) as reported in our previous study [24]. To prepare the 3BE bioink, the F127 was dissolved in 90 mL of toluene at 25 °C. Subsequently, triethylamine (TEA; Sigma 0.709 mmol, Taipei, Taiwan), 4-(dimethyl amino)-pyridine (DMAP; Sigma 0.709 mmol, Taipei, Taiwan), and 4-methacryl oxyethyl trimellitic anhydride (4-META; Sigma 1.687 mmol, Taipei, Taiwan) were added in the dissolved solution of F127. A magnetic stirring bar was employed to stir the reaction mixture at 25 °C for 16 h under a nitrogen atmosphere. The diethyl ether (Sigma, Taipei, Taiwan) was followed to add in the reaction solution to form the precipitate. The precipitate was filtered and dried with a high vacuum pressure to gain the F127-4-META. Hereafter, the F127-4-META was dissolved in 15 mL of anhydrous tetrahydrofuran (Sigma, Taipei, Taiwan) at 25 °C. the 4-(dimethylamino) pyridine (Sigma, Taipei, Taiwan), N,N′-dicyclohexylcarbodiimide (Sigma 4.650 mmol, Taipei, Taiwan), and N-hydroxysuccinimid (NHS Sigma 4.650 mmol, Taipei, Taiwan) were added in the dissolved F127-4-META. The reaction mixture was stirred with a magnetic stirring bar at 25 °C for 16 h under nitrogen atmosphere. The diethyl ether was followed to add in the reaction solution to form precipitate. The residual solvent was removed to gain the F127-4-META-NHS under a high vacuum pressure. After finishing the synthesization of F127-4-META-NHS, the triethylamine (Sigma 0.218 mmol, Taipei, Taiwan), F127-4-META-NHS, and GRGD were added in a solution contained 2.6 mL N, N-dimethylformamide (DMF; Sigma, Taipei, Taiwan). The mixed solution was stirred with a magnetic stirring bar at 25 °C for 16 h under a nitrogen atmosphere. Then, the reacted mixture solution was freeze-dried to remove the DMF. The chilled methanol was added in the reacted mixture solution without DMF to form the precipitate solution. Finally, the precipitate solution was filtered and dried to form the F127-4-META-GRGD copolymer powder (i.e., 3BE material) under a high vacuum pressure. In this study, the 3BE was prepared as various concentrations of bioink (3BE-1: 25%, 3BE-2: 30%, and 3BE-3: 35%) using culture medium for investigation.

2.2. Viscosity Measurement

The viscosity of the investigated 3BE hydrogels was measured using a RVDV-1 digital rotational viscometer (United Corps Co., Ltd, New Taipei City, Taiwan). The concentrated 3BE hydrogel with a volume of 15 mL was placed in the measuring glass and the temperature of 3BE hydrogel was kept at 25 °C. Subsequently, the spindle was moved into the concentrated 3BE hydrogel and ran with 20 rpm for 30 minutes. After finishing the measurement, the profile of the investigated hydrogel was read by RVDV-1 digital rotational viscometer. The viscosity was measured triplicates for each 3BE hydrogel (Table 1).

Table 1. Printing parameters of 3BE using self-fabricated 3D bioprinting system.

Hydrogels	Viscosity	Needle Head	Write Height	Mean Line Width	Extrudate	Lift Nozzle
	(Pa·s)	(mm)	(mm)	(mm)	(step/min)	(mm/min)
3BE-1	30 ± 0.21	0.13	0.1	0.156 ± 0.005	45	300
		0.33	0.3	0.329 ± 0.002	100	300
		0.9	0.5	0.866 ± 0.005	400	300
3BE-2	1500 ± 1.83	0.13	0.1	0.145 ± 0.008	45	300
		0.33	0.3	0.332 ± 0.001	100	300
		0.9	0.5	0.913 ± 0.001	400	300
3BE-3	$266,001,67$	0.13	0.1	0.154 ± 0.003	45	300
	$\pm 10,905$	0.33	0.3	0.336 ± 0.003	100	300
		0.9	0.5	0.931 ± 0.006	400	300

2.3. Printability Testing and Bioprinting Procedure

The protocol to generate grids and 3D complex constructs with self-fabricated 3D bioprinter was designed using the computer-aided design software (Version 2014, Dassault Systèmes SolidWorks Corp., Waltham, MA, USA). The self-fabricated 3D bioprinting system used in this study was an extruded syringe dispenser system. It means that when the dispenser is moving, the extrudates will be deposited on the platform. For printing process, we utilized the self-fabricated 3D bioprinter to print the lines using various combinations of 3BE as the bioink with three different standard needle sizes (Φ 0.13 mm, Φ 0.33 mm, and Φ 0.9 mm). Therefore, we tested nine combinations of printing parameters (Table 1). The 3D constructs were printed layer by layer (0.2 mm per layer) as the cubic-like construct (1 cm × 1 cm) with all diameters of the dispensing stainless steel needle head under the same feed rate (100 mm/s) and the dosing distance (0.06–0.08 mm). All printing procedures were performed at 37 °C. After the printing procedures, morphology characterization of the extruded lines was photographed and observed using an Olympus IX71 optical microscope (Tokyo, Japan). For bioprinting evaluation, the concentrated 3BE was placed in a 10 mL syringe and sterilized by ethylene oxide (3M 8XL, 3M, Saint Paul, MN, USA). The sterilized 3BE was followed to alter its state from solid to liquid at a temperature range of 5 °C–10 °C. Then, the L929 fibroblast cell (ATCC CCL-1, The Bioresource Collection and Research Center, Hsinchu, Taiwan) suspensions with 1×10^6 cells per mL was pipetted to the syringe. Afterward, the syringe was immediately moved to an incubator with a temperature of 37 °C for 10 minutes to form the cell-laden ink. An ideal printing combination generated from Table 1 was further adopted to investigate its post-printing cell viability.

2.4. Cell Culture

Before bioprinting, the L929 fibroblast cell line was used for cytotoxicity experiments according to ISO 10993-5 specification. The cells were thawed from a liquid nitrogen container, collected by centrifugation (1500 rpm for 5 min), and cultured in medium contained Dulbecco's modified Eagle's medium with high glucose, L-glutamine (DMEM-HG; Gibco, Taipei, Taiwan) and 10% fetal bovine serum (FBS; Gibco, Taipei, Taiwan) at 37 °C and 5% CO_2. Thereafter, the cells were maintained in 35 mm × 10 mm culture dish for seven days and the medium was replaced every three days. Once the cells reached 80% confluence, they were seeded in 96-well plate with different concentrations of 3BE-0 (0%, control), 3BE-1 (25%), 3BE-2(30%), and 3BE-3 (35%); 100 μL/well). Prior to that, cells were rinsed with phosphate-buffered saline (PBS; Sigma, Taipei, Taiwan) and detached with 0.05% trypsin–0.02% ethylenediaminetetraacetic acid (EDTA; Sigma, Taipei, Taiwan), the equal volume of medium was added to stop the trypsin-EDTA reaction. The neutralized solution was homogenously mixed and counted with hemocytometer, then cells were resuspended in the fresh medium (10 mL DMEM-HG). The cell suspensions were inoculated in each well with the same number of viable cells (1×10^3 cells/well). After that, the plate was pre-incubated in a humidified incubator (37 °C; 5% CO_2) for 24 h.

A short-term culturing experiment was utilized to evaluate its acute cytotoxicity response according to ISO 10993-5 specification.

2.5. Live/Dead Cell Assay

For quantification, the cell viability evaluation was carried out by 3-(3,4-dimethylthiazol-2-yl)-2,5-diphenyltetrazoliium bromide (MTT) assay. After 24 h of culture, the MTT solution (5 mg/mL) was prepared in PBS and filter sterilized. The 3BE was removed and 100 μL of MTT solution was added to each well. The cells were incubated for 5 h in 5% CO_2 incubator at 37 °C, during this time, the conversion of MTT resulted in purple formazan crystals. After 5 h, MTT solution was removed and 100 μL of dimethyl sulfoxide (DMSO; Sigma, Taipei, Taiwan) was added. The absorbance was measured using microplate reader (BioTek Epoch, Winooski, VT, USA) at 570 nm. The assay was performed in standard 96-well plates and each experiment was performed with nine repeats (n = 9). The results were represented as the percentage of cell viability (based on the optical density values from MTT assay).

2.6. Live/Dead Cell Observation

The cells viability inside the 3BE after printing was visualized using live/dead assay kit (Molecular Probes MP03224, Eugene, OR). The homogeneous cell encapsulation was confirmed by optical microscopy. The live/dead viability assay was performed according to the manufacturer's recommendations. Cells encapsulating 3BE hydrogel were incubated at 25 °C for 30 min in a solution of 4.0 μM ethidium homodimer-1 (EthD-1; Sigma, Taipei, Taiwan) and 2.0 μM calcein-AM (Sigma, Taipei, Taiwan) in PBS. Living cells were stained with calcein-AM (green), while dead cells were stained with EthD-1 (red). The excitation/emission filters were set at 488/530 nm to observe living cells and at 530/580 nm to detect dead cells. An Olympus IX71 fluorescence microscope was used to observe the cells. This experiment was conducted in triplicate (n = 3).

2.7. Immunofluorescence Staining

After one day and three days of culture period, the cells in the printed samples were stained with F-Actin and 4,6-diamidino-2-phenylindole (DAPI) respectively. Shortly, samples were fixed in 4% (*w/v*) paraformaldehyde for 15 min, afterwards soaked in 0.1% (*v/v*) Triton X-100 in PBS for 30 min, then blocked with 1% (*w/v*) bovine serum albumin (BSA) in PBS for 1 h at 37 °C. Then, for F-actin staining, samples were soaked in 1:40 dilution of Alexa Fluor 594-phalloidin in 0.1% (*w/v*) BSA for 45 min at 25 °C. After washing with PBS, the samples were incubated with Alexa Fluor 488 goat anti-rabbit secondary antibodies (1:200) for 1 h at 37 °C. Eventually, the nuclei were stained with DAPI (1:1000) for 5 min at 37 °C. All antibodies were diluted with 0.1% (*w/v*) BSA. To observe the cells in the final samples, an Olympus IX71 fluorescence microscope was used.

2.8. Statistical Analysis

Statistical analysis was performed with SPSS software (Version 19.0, SPSS Inc, Chicago, IL, USA). The Student *t*-test was used with $p < 0.05$ considered as significant value. All values are reported in means ± standard deviations.

3. Results

In this study, we developed a method to print hydrogel scaffolds using various combinations of 3BE and dispensing the stainless steel needle head through a self-fabricated 3D bioprinting system. First of all, we printed the combinations of 3BE-1 with different needle heads as a straight-line. It was found that the 3BE-1 with larger diameter of needle heads exhibited an irregular edge in the printed line as indicated by the arrows (Figure 1). However, the 3BE-2 or 3BE-3 with larger diameter of needle head presented a uniform edge in the printed line. Then, we tested the quality of line width after the printing process under fixed write height, extrudate, and lift nozzle. Analytical results revealed that both needle sizes and 3BE concentrations affect the quality of the printed line. Among all combinations

of printing parameters, it was found that the combination of 3BE-2 with all diameter of needle sizes produced smooth and regular line widths (Figure 2). Similar results can also be discovered in the combinations of 3BE-3. Hence, these findings reflected that both 3BE-2 and 3BE-3 combinations possessed great potential to print a stable construct.
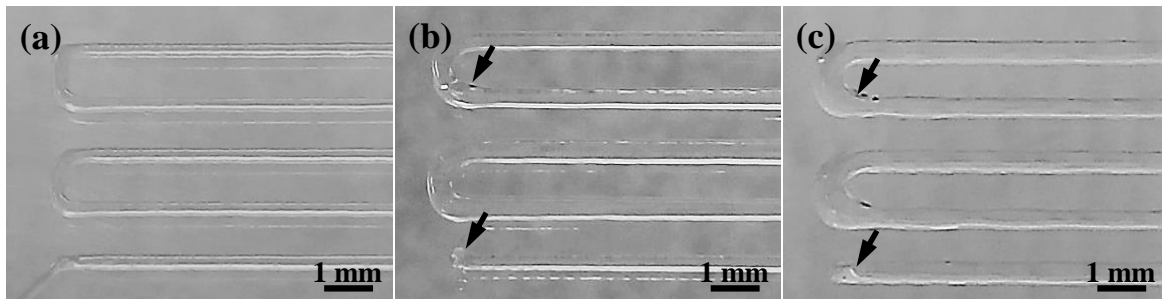

Figure 1. The combinations of 3BE-1 with different diameters of stainless steel needle heads were used to print a straight-line: (**a**) Φ 0.13 mm, (**b**) Φ 0.33 mm, and (**c**) Φ 0.9 mm.

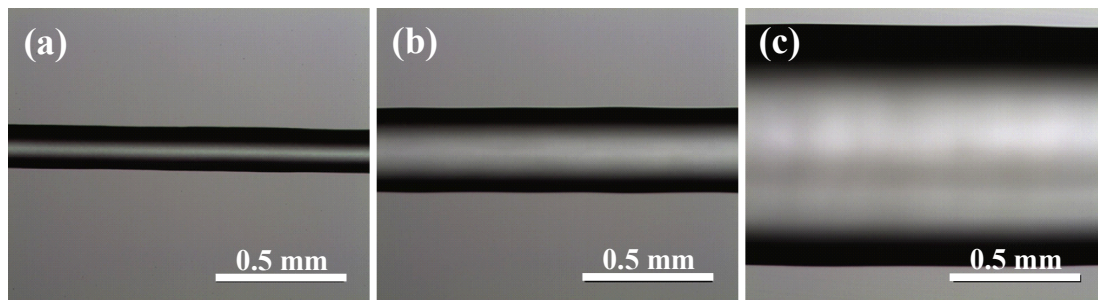**Figure 2.** The printed results from the self-fabricated 3D bioprinting system using the combinations of 3BE-2 with (**a**) Φ 0.13 mm, (**b**) Φ 0.33 mm, and (**c**) Φ 0.9 mm needle head.

Based on the abovementioned printing parameters, we then printed a more complex 3D cubic-like construct using the combinations of 3BE-2 with different needle heads. Figure 3a depicts the 3D cubic-like construct successfully printed under the combination of 3BE-2 with Φ 0.13 mm needle head. Nevertheless, we found that the generated 3D cubic-like structure collapsed after 4 h of printing even those printed samples with larger needle heads. Thus, we attempted to test the combinations of 3BE-3 according to the parameters as shown in Table 1. From this experiment, we discovered that a stable and smooth 3D cubic-like construct can be printed using the combinations of 3BE-3 (Figure 3b). Interestingly, the shape of the printed construct can be maintained for over 24 h post-printing.
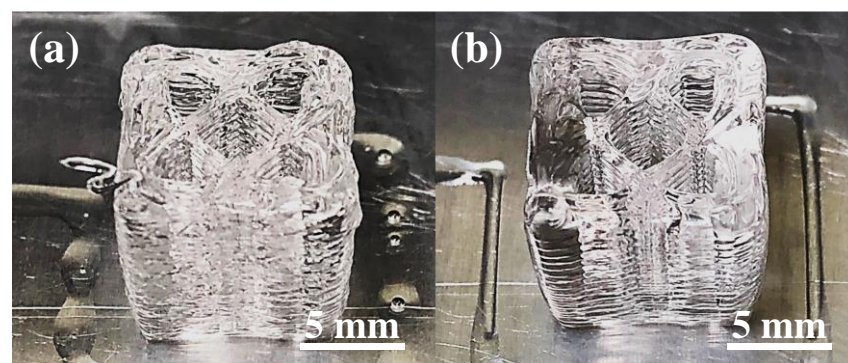

Figure 3. The 3D cubic-like constructs were printed through the self-fabricated 3D bioprinting system: (**a**) 3BE-2 combined with Φ 0.13 mm needle head and (**b**) 3BE-3 combined with Φ 0.13 mm needle head. The shape of the printed structure can be maintained for over 24 h using the combinations of 3BE-3.

In order to evaluate the biocompatibility of 3BE for cell encapsulation in 3D printing applications, firstly, we tested the cell viability of L929 fibroblast within various concentrations of 3BE in 2D monolayer. The live/dead analysis showed that more live cells were found in all 3BE groups than the dead cells (Figure 4). Among all formulations of 3BE hydrogel, the highest amount of live cells were seen in 3BE-1. In addition, we found that the cell number was rather decreased as the concentration of the 3BE increased. To confirm this result, we performed the quantitative analysis of cell viability cultured with various concentrations of 3BE shown in Figure 5. Consistent with live/dead assay, MTT analysis showed that 3BE-1 presented the highest cell viability compared to other 3BE groups and control. Even though the cell viability was decreased in 3BE-2 and 3BE-3, the number of viable cells was still above 70%, indicating the promising effect of 3BE for cell encapsulation. Based on the printability and biocompatibility results evaluation, it suggested that the ideal concentration as a bioink was 3BE-3. This concentration is further adopted for the bioprinting experiments.

After establishing idea concentration of 3BE hydrogel, we then used this concentration to print cell-laden hydrogels. Here we compiled the preliminary experiment to study the cell viability and proliferation of L929 fibroblasts within the printing process using 3BE-3 as bioink. Figure 6 shows more cell death was found after the printing procedure. Apparently, the cell viability of extrudates was significantly decreased after 24 h of printing, yet the number of live cells is still in high percentage. Data shows that the post-printing cell viability is about 50%.
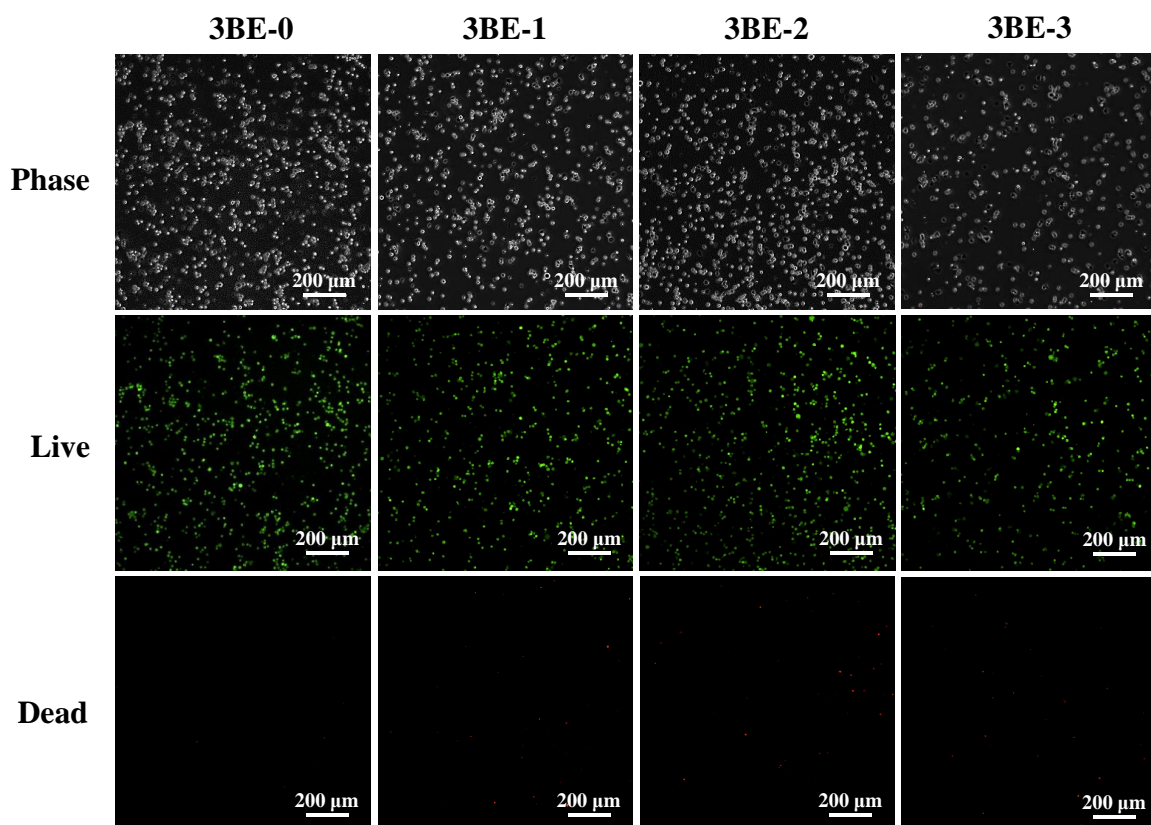

Figure 4. Live/dead analysis of cell viability in different concentrations of the 3BE before bioprinting. The green color indicates cells live and the red color indicates cells dead.
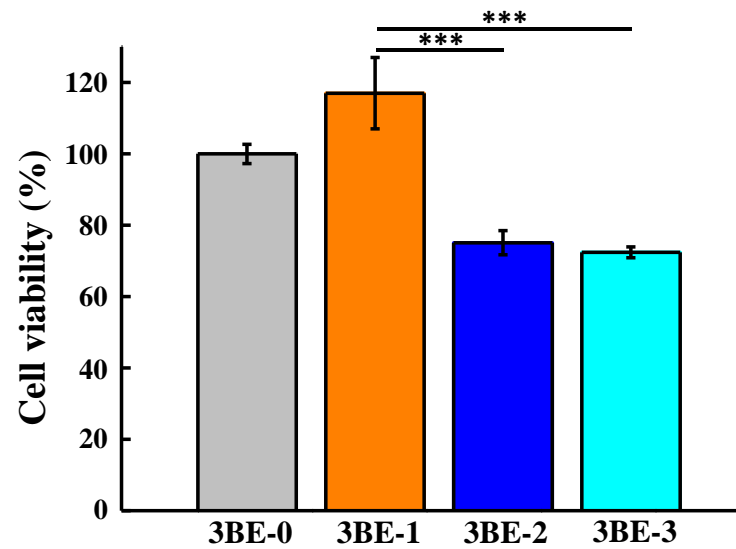
Figure 5. 3-(3,4-dimethylthiazol-2-yl)-2,5-diphenyltetrazoliium bromide (MTT) analysis for quantitative measurement of cell viability in different concentrations of the 3BE before bioprinting. The bar chart showed cell viability of L929 fibroblasts in each group was higher than 70%. The sample is considered an acute cytotoxic potential when viability value of the sample is reduced to < 70% of the blank according to ISO 109993-5. (***$p < 0.001$).
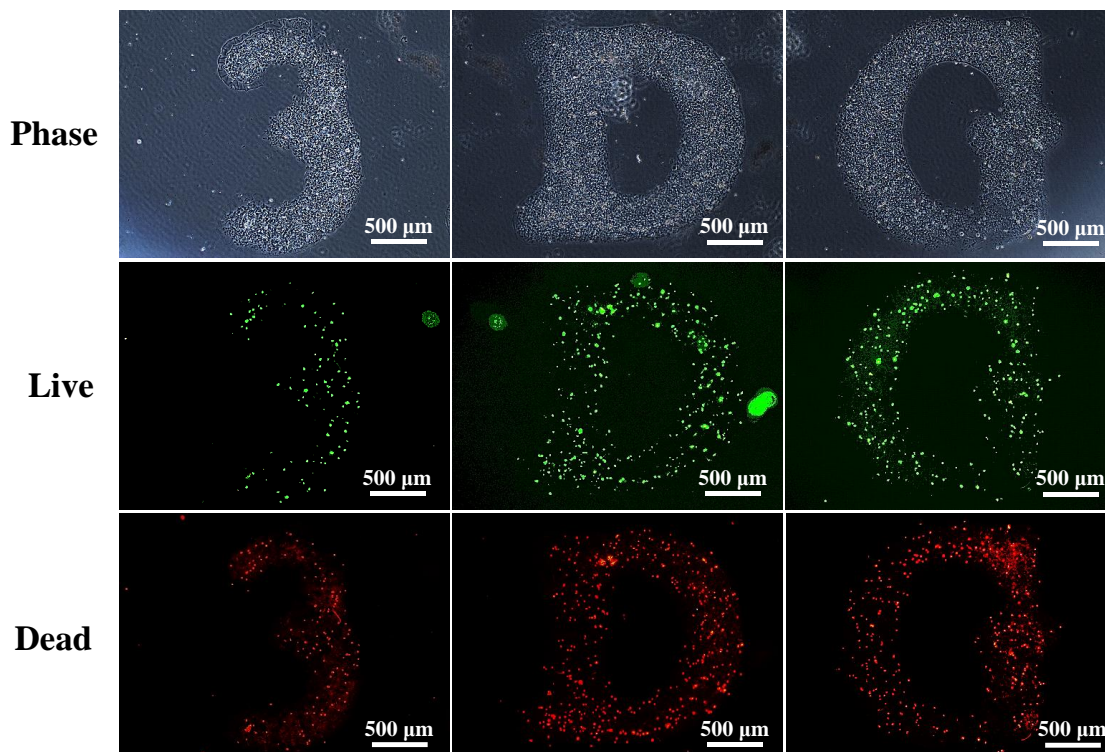

Figure 6. L929 fibroblasts bioprinted with 3BE-3 (Φ 0.13 mm needle head) hydrogel after 24 h.

Figure 7 depicts the immunofluorescence staining of L929 fibroblasts to further evaluate 3BE-3 bioink for supporting cell proliferation after bioprinting. Images showed that L929 fibroblasts were able to attach on the 3BE surface on day one of culture. Furthermore, after three days of culture, the immunofluorescence results showed that L929 fibroblasts were fused and alive. This data indicated that the cells have significant proliferation inside

the 3BE-3 within three days after bioprinting. These features can also be discovered in the bioprinted 3BE-3 combinations with larger needle heads (Φ 0.33 mm and Φ 0.9 mm).
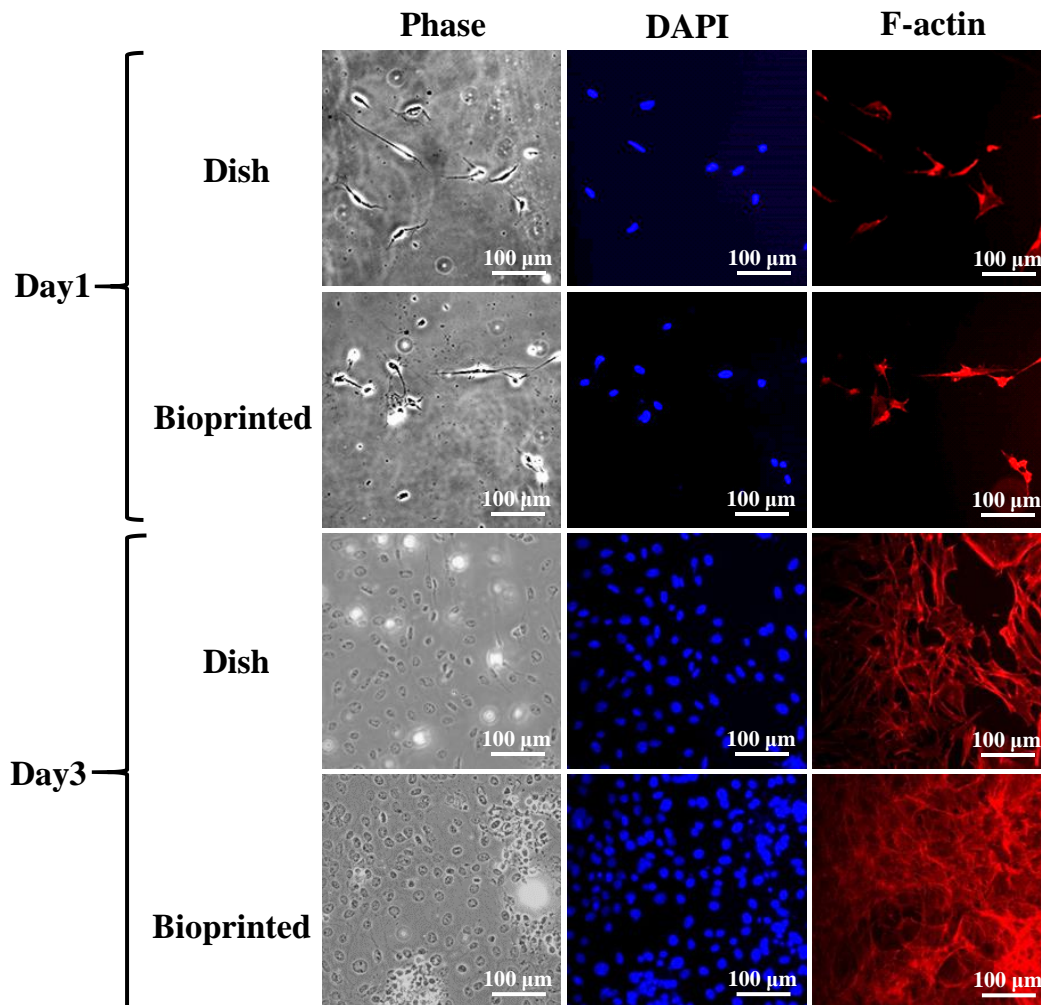

Figure 7. Cell proliferation of L929 fibroblasts in the 3BE-3 (Φ 0.13 mm needle head) at days one and three after bioprinting. More cell proliferation was seen in day three compared to day one.

4. Discussion

In order to create complex tissue/organ structure using 3D bioprinting technology, the printability of hydrogel is a crucial aspect to allow for a suitable environment for organ functionalizations [19,29]. When applying specific materials for bioink in micro-extrusion printing, an appropriate printing parameter should be considered to achieve optimum printing structures [28]. In this study, we presented a preliminary ideal index of 3BE hydrogel as bioink to generate complex 3D architectures by means of self-fabricated 3D bioprinting system. We found that different combinations of printing parameters, especially the needle size and bioink concentration influence the printed results.

The biomaterial properties and biological requirements of bioink may affect their performances in 3D bioprinting applications [10]. In the present study, we observed the printing quality of line width after the printing process using 3BE-1 hydrogel under fixed needle sizes, yet we found that the 3D construct cannot be printed in all combinations made. This may be due to the low concentration of 3BE hydrogel being used. A previous study found that the 3D bioprinting accuracy of hydrogels depends largely on polymer concentrations [30]. Low viscosities of bioink often failed to generate the 3D printing of layers [31]. Fortunately, the printability and properties of the resulting 3D constructs can

be significantly improved by changing the concentration of the components [27]. In this study, we discovered a slight increase in the printing quality of line width when 3BE-2 or 3BE-3 was used compared to 3BE-1. In addition, the image taken after printing the line using the 3BE-2 and 3BE-3 hydrogels indicated that both concentrations could be the ideal option to generate a precise and stable line width.

Regarding the 3D construct from the printing parameter, we observed that the intended shape can be printed using the combinations of 3BE-2. However, the printed constructs with the 3BE-2 combinations failed after 4 h post-printing. This feature implied that the viscosity in this range (~1500 Pa·s) cannot be applied to support the 3D construct. Whereas, in order to bioprint a stable soft tissue structure, the combinations of 3BE-3 hydrogel might be the ideal options. We found that when using these combinations, a stable and smooth 3D construct can be generated. The F127 content in the composite highly influences the printability of the hydrogel. The higher the concentration of F127 hydrogel, the better printability can be reached [19]. Altering appropriate concentration ratios of gelatin and hydrogel could generate regular and smooth fibers steadily resulting in excellent printability [32].

Furthermore, we also compiled the preliminary experiment to study the viability of L929 fibroblasts combined with 3BE hydrogel within the printing process. It was found that more cell death was present 24 h post-printing. The decrease of cell viability after printing is the commonly encountered issues in 3D bioprinting application [33]. This might be caused by the pressure used to expel the bioink in microextrusion bioprinting [34]. Printing at higher extrusion pressures will increase the number of dead cells since a higher pressure will elevate the shear stress in the nozzle, which eventually damages the cell membrane and leads to lower cell viability after extrusion [21,35]. A previously published study demonstrated an inverse relationship between extrusion pressure and cellular viability, especially in high extrusion pressures [34]. In addition, hydrogel concentrations can be another issue to affect cell viability after printing. One study found that a higher concentration of hydrogel showed the fastest decrease in metabolic activity of the cell compared to the low concentration group in long term observation [36].

In the present study, we found that L929 fibroblasts were alive and proliferated over three days in the 3BE-3 combinations, pointing that 3BE-3 hydrogel might be a favorable material to stimulate cell growth and proliferation when formulated for cell-encapsulation in 3D bioprinting. As suggested from previous studies, the thermo-responsive properties of this hydrogel evinced them as attractive biomaterials for cell encapsulation and cell delivery scaffold [37]. Future targets of this study were distinguishing the best 3BE hydrogel to mix with other biomaterials such as bone graft for creating an intended porosity of scaffold through the 3D printing procedure. Since in this study, we only investigated the bioink viscosity and needle size for printing the 3D constructs, thus, future investigation regarding the viscosity property, printing time, printing speed, pressure, and nozzle size which possibly influence the printed result is strongly recommended to obtain the optimum output from 3D bioprinting procedure.

5. Conclusions

In this study, we have reported a potential printing parameter of the 3BE hydrogel that offers stable printability, solid configuration, and biocompatibility for 3D bioprinting. The investigated results represent the extensive potential of 3BE hydrogel as a bioink to generate an ideal 3D printed result. Besides, this material could promote both cell growth and proliferation after the printing procedure. Further, this finding could serve as a new strategy to create a complex configuration of a functional scaffold for 3D bioprinting and tissue engineering applications.

Author Contributions: Investigation, S.-Y.C. and Y.-C.C. (Yung-Chieh Cho).; methodology, B.-H.H.; data curation, W.-C.L. C.-H.T. and H.-W.C.; supervision; C.J.W. and T.S.; validation, T.-S.Y. and M.R.; visuali-zation, Y.-C.C. (Yen-Chun Chuo). and H.-Y.L.; writing—original draft, S.-Y.C.; writing—

References

1. Aljohani, W.; Ullah, M.W.; Zhang, X.; Yang, G. Bioprinting and its applications in tissue engineering and regenerative medicine. *Int. J. Biol. Macromol.* **2018**, *107*, 261–275. [CrossRef] [PubMed]

2. Bittner, S.M.; Guo, J.L.; Mikos, A.G. Spatiotemporal control of growth factors in three-dimensional printed scaffolds. *Bioprinting* **2018**, *12*, e00032. [CrossRef] [PubMed]

3. Celikkin, N.; Simó Padial, J.; Costantini, M.; Hendrikse, H.; Cohn, R.; Wilson, C.J.; Rowan, A.E.; Święszkowski, W. 3D printing of thermoresponsive polyisocyanide (pic) hydrogels as bioink and fugitive material for tissue engineering. *Polymers* **2018**, *10*, 555. [CrossRef] [PubMed]

4. Garreta, E.; Oria, R.; Tarantino, C.; Pla-Roca, M.; Prado, P.; Fernandez-Aviles, F.; Campistol, J.M.; Samitier, J.; Montserrat, N. Tissue engineering by decellularization and 3D bioprinting. *Mater. Today* **2017**, *20*, 166–178. [CrossRef]

5. Jia, W.; Gungor-Ozkerim, P.S.; Zhang, Y.S.; Yue, K.; Zhu, K.; Liu, W.; Pi, Q.; Byambaa, B.; Dokmeci, M.R.; Shin, S.R. Direct 3D bioprinting of perfusable vascular constructs using a blend bioink. *Biomaterials* **2016**, *106*, 58–68. [CrossRef]

6. Bittner, S.M.; Guo, J.L.; Melchiorri, A.; Mikos, A.G. Three-dimensional printing of multilayered tissue engineering scaffolds. *Mater. Today* **2018**, *21*, 861–874. [CrossRef]

7. Datta, P.; Barui, A.; Wu, Y.; Ozbolat, V.; Moncal, K.K.; Ozbolat, I.T. Essential steps in bioprinting: From pre-to post-bioprinting. *Biotechnol. Adv.* **2018**, *36*, 1481–1504. [CrossRef]

8. Malda, J.; Visser, J.; Melchels, F.P.; Jüngst, T.; Hennink, W.E.; Dhert, W.J.; Groll, J.; Hutmacher, D.W. 25th anniversary article: Engineering hydrogels for biofabrication. *Adv. Mater.* **2013**, *25*, 5011–5028. [CrossRef]

9. Murphy, S.V.; Skardal, A.; Atala, A. Evaluation of hydrogels for bio-printing applications. *J. Biomed. Mater. Res. Part A* **2013**, *101*, 272–284. [CrossRef]

10. Noh, I.; Kim, N.; Tran, H.N.; Lee, J.; Lee, C. 3D printable hyaluronic acid-based hydrogel for its potential application as a bioink in tissue engineering. *Biomater. Res.* **2019**, *23*, 3. [CrossRef]

11. Hospodiuk, M.; Dey, M.; Sosnoski, D.; Ozbolat, I.T. The bioink: A comprehensive review on bioprintable materials. *Biotechnol. Adv.* **2017**, *35*, 217–239. [CrossRef] [PubMed]

12. Williams, D.; Thayer, P.; Martinez, H.; Gatenholm, E.; Khademhosseini, A. A perspective on the physical, mechanical and biological specifications of bioinks and the development of functional tissues in 3D bioprinting. *Bioprinting* **2018**, *9*, 19–36. [CrossRef]

13. Panwar, A.; Tan, L.P. Current status of bioinks for micro-extrusion-based 3D bioprinting. *Molecules* **2016**, *21*, 685. [CrossRef] [PubMed]

14. Skardal, A.; Devarasetty, M.; Kang, H.-W.; Mead, I.; Bishop, C.; Shupe, T.; Lee, S.J.; Jackson, J.; Yoo, J.; Soker, S. A hydrogel bioink toolkit for mimicking native tissue biochemical and mechanical properties in bioprinted tissue constructs. *Acta Biomater.* **2015**, *25*, 24–34. [CrossRef] [PubMed]

15. Shahin-Shamsabadi, A.; Selvaganapathy, P.R. Excel: Combining extrusion printing on cellulose scaffolds with lamination to create in vitro biological models. *Biofabrication* **2019**, *11*, 035002. [CrossRef] [PubMed]

16. Webb, B.; Doyle, B.J. Parameter optimization for 3D bioprinting of hydrogels. *Bioprinting* **2017**, *8*, 8–12. [CrossRef]

17. Chang, C.C.; Boland, E.D.; Williams, S.K.; Hoying, J.B. Direct-write bioprinting three-dimensional biohybrid systems for future regenerative therapies. *J. Biomed. Mater. Res. Part B Appl. Biomater.* **2011**, *98*, 160–170. [CrossRef]

18. Kolesky, D.B.; Truby, R.L.; Gladman, A.S.; Busbee, T.A.; Homan, K.A.; Lewis, J.A. 3D bioprinting of vascularized, heterogeneous cell-laden tissue constructs. *Adv. Mater.* **2014**, *26*, 3124–3130. [CrossRef]

19. Suntornnond, R.; Tan, E.Y.S.; An, J.; Chua, C.K. A highly printable and biocompatible hydrogel composite for direct printing of soft and perfusable vasculature-like structures. *Sci. Rep.* **2017**, *7*, 1–11. [CrossRef]

20. Gioffredi, E.; Boffito, M.; Calzone, S.; Giannitelli, S.M.; Rainer, A.; Trombetta, M.; Mozetic, P.; Chiono, V. Pluronic f127 hydrogel characterization and biofabrication in cellularized constructs for tissue engineering applications. *Procedia Cirp* **2016**, *49*, 125–132. [CrossRef]

21. Fakhruddin, K.; Hamzah, M.S.A.; Razak, S.I.A. *Effects of Extrusion Pressure and Printing Speed of 3D Bioprinted Construct on the Fibroblast Cells Viability*; IOP Conference Series: Materials Science and Engineering; IOP Publishing: Bristol, UK, 2018; p. 012042.

22. Deidda, G.; Jonnalagadda, S.V.R.; Spies, J.W.; Ranella, A.; Mossou, E.; Forsyth, V.T.; Mitchell, E.P.; Bowler, M.W.; Tamamis, P.; Mitraki, A. Self-assembled amyloid peptides with arg-gly-asp (rgd) motifs as scaffolds for tissue engineering. *ACS Biomater. Sci. Eng.* **2017**, *3*, 1404–1416. [CrossRef] [PubMed]

23. Dumbleton, J.; Agarwal, P.; Huang, H.S.; Hogrebe, N.; Han, R.Z.; Gooch, K.J.; He, X.M. The effect of rgd peptide on 2D and miniaturized 3D culture of hepm cells, mscs, and adscs with alginate hydrogel. *Cell Mol. Bioeng* **2016**, *9*, 277–288. [CrossRef] [PubMed]

24. Cho, Y.C.; Huang, H.T.; Lan, W.C.; Huang, M.S.; Saito, T.; Huang, B.B.; Tsai, C.H.; Fang, F.Y.; Ou, K.L. The Potential of a Tailored Biomimetic Hydrogel for In Vitro Cell Culture Applications: Characterization and Biocompatibility. *Appl. Sci.* **2020**, *10*, 9035. [CrossRef]

25. Re'em, T.; Tsur-Gang, O.; Cohen, S. The effect of immobilized rgd peptide in macroporous alginate scaffolds on tgf beta 1-induced chondrogenesis of human mesenchymal stem cells. *Biomaterials* **2010**, *31*, 6746–6755. [CrossRef] [PubMed]

26. Lecarpentier, Y.; Kindler, V.; Bochaton-Piallat, M.L.; Sakic, A.; Claes, V.; Hebert, J.L.; Vallee, A.; Schussler, O. Tripeptide arg-gly-asp (rgd) modifies the molecular mechanical properties of the non-muscle myosin iia in human bone marrow-derived myofibroblasts seeded in a collagen scaffold. *PLoS ONE* **2019**, *14*, e0222683. [CrossRef]

27. Derakhshanfar, S.; Mbeleck, R.; Xu, K.; Zhang, X.; Zhong, W.; Xing, M. 3D bioprinting for biomedical devices and tissue engineering: A review of recent trends and advances. *Bioact. Mater.* **2018**, *3*, 144–156. [CrossRef]

28. Abdollahi, S.; Davis, A.; Miller, J.H.; Feinberg, A.W. Expert-guided optimization for 3D printing of soft and liquid materials. *PLoS ONE* **2018**, *13*, e0194890. [CrossRef]

29. Costantini, M.; Idaszek, J.; Szöke, K.; Jaroszewicz, J.; Dentini, M.; Barbetta, A.; Brinchmann, J.E.; Święszkowski, W. 3D bioprinting of bm-mscs-loaded ecm biomimetic hydrogels for in vitro neocartilage formation. *Biofabrication* **2016**, *8*, 035002. [CrossRef]

30. Wang, X. Advanced polymers for three-dimensional (3D) organ bioprinting. *Micromachines* **2019**, *10*, 814. [CrossRef]

31. Roopavath, U.K.; Malferrari, S.; Van Haver, A.; Verstreken, F.; Rath, S.N.; Kalaskar, D.M. Optimization of extrusion based ceramic 3D printing process for complex bony designs. *Mater. Des.* **2019**, *162*, 263–270. [CrossRef]

32. Yin, J.; Yan, M.; Wang, Y.; Fu, J.; Suo, H. 3D bioprinting of low-concentration cell-laden gelatin methacrylate (gelma) bioinks with a two-step cross-linking strategy. *Acs Appl. Mater. Interfaces* **2018**, *10*, 6849–6857. [CrossRef] [PubMed]

33. Ning, L.; Chen, X. A brief review of extrusion-based tissue scaffold bio-printing. *Biotechnol. J.* **2017**, *12*, 1600671. [CrossRef] [PubMed]

34. Bishop, E.S.; Mostafa, S.; Pakvasa, M.; Luu, H.H.; Lee, M.J.; Wolf, J.M.; Ameer, G.A.; He, T.-C.; Reid, R.R. 3-d bioprinting technologies in tissue engineering and regenerative medicine: Current and future trends. *Genes Dis.* **2017**, *4*, 185–195. [CrossRef] [PubMed]

35. You, F.; Eames, B.F.; Chen, X. Application of extrusion-based hydrogel bioprinting for cartilage tissue engineering. *Int. J. Mol. Sci.* **2017**, *18*, 1597. [CrossRef] [PubMed]

36. Wang, L.L.; Highley, C.B.; Yeh, Y.C.; Galarraga, J.H.; Uman, S.; Burdick, J.A. Three-dimensional extrusion bioprinting of single-and double-network hydrogels containing dynamic covalent crosslinks. *J. Biomed. Mater. Res. Part A* **2018**, *106*, 865–875. [CrossRef] [PubMed]

37. Diniz, I.M.; Chen, C.; Xu, X.; Ansari, S.; Zadeh, H.H.; Marques, M.M.; Shi, S.; Moshaverinia, A. Pluronic f-127 hydrogel as a promising scaffold for encapsulation of dental-derived mesenchymal stem cells. *J. Mater. Sci. Mater. Med.* **2015**, *26*, 153. [CrossRef]